Magnetic-Field Transducer Based on Closed-Loop Operation of Magnetic Sensors

Gabriele Grandi, *Member, IEEE*, and Marco Landini

***Abstract*—A high-sensitivity magnetic transducer able to sense magnetic fields from dc up to tens of kilohertz is analyzed in this paper. The system is based on a nulling field coil fed by a current on the basis of the residual field, sensed by a magnetic sensor (Hall or magnetoresistive) placed in the coil center. In this way, the coil current proportionally represents the external field component along the coil axis, and it can be easily converted in a voltage signal by a series resistor. Then, a one-axis Gauss meter can be readily obtained. The sensitivity and the bandwidth of the overall system are discussed by a transfer function analysis. A hardware prototype has been realized, and significant test results are shown by means of a reference magnetic-field-generation setup. Useful guidelines for the overall system design are given.**

***Index Terms*—Hall devices, magnetic measurements, magnetic transducers, magnetoresistive devices.**

I. Introduction

RECENTLY, additional research and public attention have been focused on possible health effects of low-frequency magnetic fields, with reference to low-level long-period human exposures. Furthermore, the measurement of magnetic field has become an important concern in industry over the past several years. As a consequence, scientific and technical attention has been directed to the development of apparatus and protocol to accurately sense and measure magnetic fields [1]. The challenge is to realize magnetic transducers, or Gauss meters, having at the same time high sensitivity, good accuracy, and wide bandwidth, with the additional requirement to be economically feasible.

Conventional field-measurement technologies [2], [3] mainly include integrating flux meters (based on Faraday's law), flux-gate magnetometers [4], and open-loop magnetic sensors [5]. The use of Hall-effect sensors and magnetoresistive devices has been recently encouraged by the development of hardware and software compensation blocks to improve the system accuracy. In fact, these sensing elements are inherently nonlinear [6], and they are affected by field strength and temperature. Then, a thermistor is required as additional component. Various compensation methods have been considered, such as mathematical models and polynomial approximations. More recently, erasable programmable ROM (EPROM) data storage [7] and artificial neural network [8] have been proposed. In general, these methods exhibit good results but require sophisticated instrumentation amplifiers, digital signal processors, and a laborious tuning or learning process.

Manuscript received December 12, 2002; revised June 17, 2005. Abstract published on the Internet March 18, 2006.

The authors are with the Department of Electrical Engineering University of Bologna, 40141 Bologna, Italy (e-mail: gabriele.grandi@mail.ing.unibo.it).

Digital Object Identifier 10.1109/TIE.2006.874277

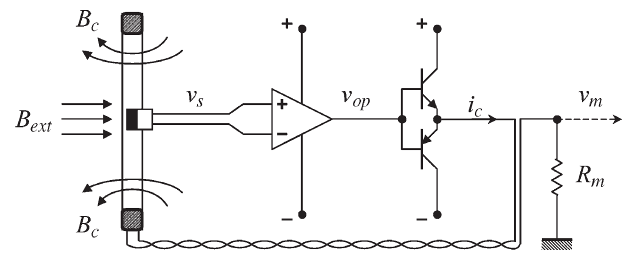

Fig. 1. Simplified circuit diagram of the system.

In order to overcome these drawbacks, a closed-loop magnetic transducer based on nulling the field across the magnetic sensor is considered in this paper. The current flowing in the nulling coil is driven by the sensor signal. In this way, the sensor is kept inside the control loop and, if the loop gain is high enough, the coil current is proportional to the magnetic field, regardless of the sensor nonlinearities and temperature drifts. The transducer circuit is described with additional details in Section II whereas the transducer behavior is characterized in Section III by a transfer-function analysis. Section IV summarizes a comparison with respect to other magnetic transducers. Some practical results are presented in Section V, on the basis of an experimental setup including a transducer prototype and a reference magnetic-field-generation system.

II. Circuit Description

A simplified circuit diagram of the closed-loop magnetic-field transducer is shown in Fig. 1. The magnetic sensor (Hall or magnetoresistive) is placed in the coil center. It produces a voltage ν_s proportional to the residual flux density along the coil axes

$$\nu_s = K_\mathrm{s}\Delta B = K_\mathrm{s}(B_\mathrm{ext} - B_\mathrm{co}) \tag{1}$$

B_ext being the external magnetic-flux density and B_co the magnetic-flux density generated by the compensating current i_c in the coil center.

The parameter K_s represents the open-circuit sensitivity of the magnetic sensor.

The sensor voltage is amplified by an op-amp that feeds a push–pull amplifier. The push–pull amplifier drives the coil current i_c in order to cancel the magnetic field in the coil center. The resulting working point, near zero field, eliminates the dependence on the linearity of the magnetic sensor and also reduces the temperature drift, as shown in the next section.

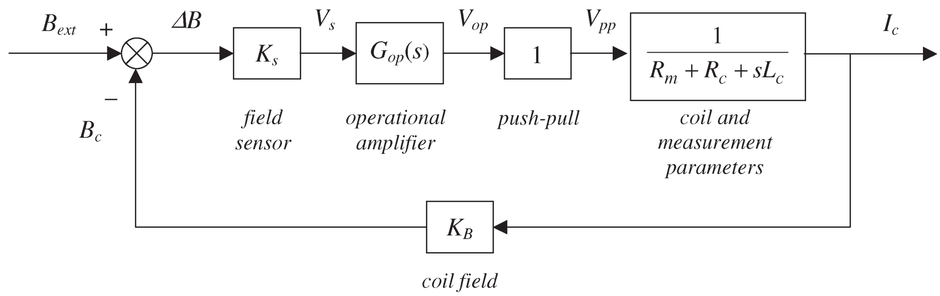

Fig. 2. Block diagram of the closed-loop magnetic transducer.

The output current is converted to the voltage ν_m by placing the measurement resistor $R_{\rm m}$ from the coil to ground.

The nulling coil consists of an air-core winding having N_c turns, with a coil resistance $R_{\rm c}$ and a coil inductance $L_{\rm c}$. The relationship between $i_{\rm c}$ and $B_{\rm co}$ is given by the field coefficient K_B, defined as

$$K_B = \frac{B_o}{i_{\rm c}}. \tag{2}$$

With reference to a circular winding shaped as a ring, if the coil diameter $D_{\rm c}$ is expressed in millimeters, the field coefficient can be expressed in microtesla per milliampere as

$$K_B \cong 0.4\pi \frac{N_{\rm c}}{D_{\rm c}} (\mu\text{T/mA}). \tag{3}$$

III. Transfer Function Analysis

The block diagram of the overall system is represented in Fig. 2, assuming the nulling coil current $i_{\rm c}$ as the output and the external field $B_{\rm ext}$ as the input variable. The resulting closed-loop transfer function, representing a current sensitivity (milliampere per microtesla), can be expressed as

$$\frac{i_{\rm c}(s)}{B_{\rm ext}(s)} = S_{\rm I}(s) = \frac{G(s)}{1+G(s)H(s)} = \frac{1}{H(s)+1/G(s)} \tag{4}$$

where

$$G(s) = \frac{K_{\rm s} G_{\rm op}(s)}{R_{\rm m}+R_{\rm c}+sL_{\rm c}} = \frac{K_{\rm s}}{R_{\rm tot}} \frac{G_{\rm op}(s)}{(1+\tau_c s)}, \qquad \tau_c = \frac{L_{\rm c}}{R_{\rm tot}} \tag{5}$$

$$H(s) = K_B. \tag{6}$$

It is assumed that the sensor bandwidth (which is usually in the range of megahertz) is much greater with respect to those of the other blocks. Then, the sensor dynamic is neglected and the corresponding sensor sensitivity $K_{\rm s}$ is treated as a real number. The op-amp can be considered as a first-order system to represent its open-loop behavior

$$G_{\rm op}(s) = \frac{K_{\rm op}}{1+\tau_{\rm op} s} \tag{7}$$

where $K_{\rm op}$ is the static gain, and $\tau_{\rm op}$ is the time constant (open loop). Usually, $\tau_{\rm op}$ is in the order of tens of milliseconds, much greater than τ_c, which is in the order of tens of microseconds

$$\tau_{\rm op} \gg \tau_c. \tag{8}$$

On the basis of (8), it can be assumed that the op-amp pole expressed in (7) dominates with respect to the coil pole expressed in (5). Then, as a first order of approximation, the coil dynamic can be neglected, and (5) can be simplified as

$$G(s) \cong \frac{K_{\rm s} K_{\rm op}}{R_{\rm tot}} \frac{1}{1+\tau_{\rm op} s}. \tag{9}$$

Introducing (9) and (6) in (4), a simplified first-order transfer function is obtained for the magnetic transducer

$$S_{\rm I}(s) \cong \frac{1}{K_B + \frac{R_{\rm tot}}{K_{\rm s} K_{\rm op}} (1+\tau_{\rm op} s)}. \tag{10}$$

Equation (10) can be rewritten in terms of static gain $S_{\rm I}(0)$ and time constant τ of the overall system (closed loop)

$$S_{\rm I}(s) \cong \frac{S_{\rm I}(0)}{1+\tau s} \tag{11}$$

where

$$S_{\rm I}(0) = \frac{1/K_B}{1+\frac{R_{\rm tot}}{K_B K_{\rm s} K_{\rm op}}} \quad \text{and} \quad \tau = \frac{\tau_{\rm op}}{1+\frac{K_B K_{\rm s} K_{\rm op}}{R_{\rm tot}}}. \tag{12}$$

It will be shown later that the loop static gain $K_{\rm tot}$ is much greater than one

$$K_{\rm tot} = G(0)H(0) = \frac{K_B K_{\rm s} K_{\rm op}}{R_{\rm tot}} \gg 1. \tag{13}$$

Then, (12) is further simplified as

$$S_{\rm I}(0) \cong \frac{1}{K_B}, \qquad \tau \cong \frac{\tau_{\rm op}}{K_{\rm tot}} \quad \text{or} \quad f_o \cong K_{\rm tot} f_{\rm op}. \tag{14}$$

The static and dynamic characteristics of the magnetic transducer are expressed in (11) and (14), and can be summarized in two main points.

1) The static gain $S_{\rm I}(0)$ represents the current sensitivity in terms of milliampere per microtesla. $S_{\rm I}(0)$ is an inverse function of the field coefficient K_B, i.e., it depends on the geometrical characteristic of the nulling coil only.
As a consequence, $S_{\rm I}(0)$ can be expressed as $1/K_B$, e.g., by (3), regardless of nonlinearity or thermal drift affecting

the open-circuit sensitivity coefficient K_s of the magnetic sensor.

2) The cutoff frequency f_o, representing the bandwidth of the magnetic transducer, is K_tot times the open-loop cutoff frequency of the op-amp f_op, as shown in (14).

In particular, (13) shows that the lower is the total resistance R_tot, the higher is K_tot and the bandwidth. On the other hand, the measuring resistance R_m should be high enough to have a good output-voltage resolution.

The value of K_B should be chosen by a compromise also: It is advisable to be high enough to obtain a wide bandwidth, but it should be limited to have a good current sensitivity in terms of milliampere per microtesla.

The static gain can be represented in terms of output-voltage sensitivity $S_\mathrm{V}(0)$, expressed in millivolt per microtesla, as

$$S_\mathrm{V}(0) = R_\mathrm{m} S_\mathrm{I}(0) \cong R_\mathrm{tot} S_\mathrm{I}(0) = \frac{R_\mathrm{tot}}{K_B}. \quad (15)$$

Then, it is useful to introduce a "gain-bandwidth product" (GBP) for the magnetic transducer, as the product between the voltage sensitivity and the closed-loop cutoff frequency

$$\mathrm{GBP_V} = S_\mathrm{V}(0) \cdot f_o \cong \frac{R_\mathrm{tot}}{K_B} \cdot K_\mathrm{tot} f_\mathrm{op} = K_\mathrm{s} \cdot K_\mathrm{op} f_\mathrm{op}. \quad (16)$$

By introducing in (16) the GBP for the op-amp, we arrive at

$$\mathrm{GBP_V} \cong K_\mathrm{s} \cdot \mathrm{GBP_{op}}. \quad (17)$$

Equation (17) states that the overall $\mathrm{GBP_V}$ of the closed-loop magnetic transducer is practically affected only by the open-circuit sensitivity of the magnetic sensor, and the GPB of the op-amp. Increasing the sensitivity decreases the bandwidth or vice versa.

IV. Comparison With Respect to Other Magnetic-Field Transducers

As known, the operating principle of integrating flux meters is based on Faraday's law of induction. As a consequence, the flux meters require a very stable integrator to obtain the magnetic field with a good accuracy, starting from the voltage induced on a coil probe. The main advantage of the magnetic-field transducers based on Hall-effect or magnetoresistive sensors with respect to integrating flux meters is the possibility to accurately sense extremely low frequency, including dc fields. In addition, magnetic sensor can be moved during the measurements, whereas the coil probe of the flux meters must stand still to avoid induced voltage perturbations.

The main advantage of the proposed closed-loop transducer with respect to the open-loop ones is to overcome the problems related to the compensation of nonlinear behavior and thermal drift of the magnetic sensor element. Then, the closed-loop system leads to higher stability, better accuracy and reduced costs. On the other hand, the proposed system introduces a field perturbation in the region around the transducer, due to the compensating current through the nulling coil. As an example, in the case of circular coils shaped as a ring, the disturbance field B_d can be approximated by the expression of the magnetic flux density at the distance d far from a circular current loop

$$B_d \cong 0.05\pi D_\mathrm{c}^2 \frac{N_c i_\mathrm{c}}{d^3}, \qquad (\mu\mathrm{T}) \quad \text{with} \quad d \gg D_\mathrm{c}. \quad (18)$$

With reference to a uniform external field B_ext, the compensating field generated by the coil in the coil center is $B_o = B_\mathrm{ext}$. Then, considering (2), (3), and (18), the ratio between the disturbance field B_d and the uniform external field B_ext, i.e., the measured one, is determined as

$$\frac{B_d}{B_\mathrm{ext}} \cong \frac{1}{8}\left(\frac{D_\mathrm{c}}{d}\right)^3. \quad (19)$$

Equation (19) shows that the relative field disturbance is about 0.1% at a distance d only five times greater than the coil diameter D_c. It can be noted that the sensitivity of the proposed closed-loop transducer is slightly affected by ferromagnetic objects in the close proximity of the nulling coil, due to the variation in the field coefficient K_B. These perturbations are negligible if the distance of the ferromagnetic objects from the nulling coil is larger with respect to their geometric dimensions.

V. Experimental Setup and Results

Significant experimental tests carried out on a measuring-system prototype are presented in this section. An implementation of the closed-loop magnetic transducer is described in Section V-A, together with some practical considerations. A reference magnetic-field-generation system able to generate the testing field is described in Section V-B. The experimental results are presented in Section V-C, emphasizing the static and the dynamic characteristic of the magnetic transducer prototype.

A. Magnetic-Transducer-Prototype Description

A magnetic-transducer prototype has been realized on the basis of the specific guidelines given in Section III. Two windings with a different number of turns have been wound: The coil #1 has $N_c = 10$; the coil #2 has $N_c = 50$. The main geometric and electric parameters are given in Table I.

In order to emphasize the prototype behavior in its whole frequency range, it has been chosen to limit the bandwidth to a few kilohertz, since the magnetic-field-generation system covers a frequency range up to 5 kHz (see Section V-B).

In Table II are reported main static and dynamic parameters of the magnetic transducer, calculated by the expressions given in Section III.

Having the static gain of the op-amp high enough, it is verified that the loop static gain is $K_\mathrm{tot} \gg 1$, as previously stated in Section III. Then, the current sensitivity $S_\mathrm{I}(0)$ of the closed-loop magnetic transducer is a function of the field coefficient K_B only.

TABLE I
ELECTRIC AND GEOMETRIC PROTOTYPE PARAMETERS

Parameters	*Symbols*	*Values*	*Units*
Coils		#1 / #2	
Diameter	D_c	53 / 50.5	mm
Turns number	N_c	10 / 50	
Resistance	R_c	1.2 / 5.7	Ω
Inductance	L_c	12 / 280	μH
Op-amp characteristics (rated, open-loop)			
Cut-off frequency	f_{op}	25	Hz
Static gain	K_{op}	106	dB
Gain BW Product	GBP_{op}	5000	kHz
Circuit and sensor parameters (rated)			
Measuring resistance	R_m	100	Ω
Power supply	E_{dc}	± 12	V
Sensor type		magneto-resistive	
Open circuit sensitivity	K_s	0.045 ÷ 0.106	mV/μT
Frequency range	f_s	0 to 1M	Hz

TABLE II
STATIC AND DYNAMIC PROTOTYPE PARAMETERS

Parameters	*Symbols*	*Coil* #1	*Coil* #2	*Units*
Field coeff.	K_B	0.238	1.247	μT/mA
Loop gain	K_{tot}	21 ÷ 50	106 ÷ 250	-
Cut-off freq.	f_o	0.5 ÷ 1.2	2.6 ÷ 6.2	kHz
Current sens.	$S_I(0)$	4.2	0.80	mA/μT
Voltage sens.	$S_V(0)$	420	80	mV/μT
GBP (voltage)	GBP_V	210 ÷ 500	210 ÷ 500	kHz mV/μT

B. Reference-Field-Generation System

A reference magnetic-field-generation system has been realized in order to verify static and dynamic performances of the transducer prototype. In particular, a square Helmholtz coil has been built by a solid-wood structure, assembled with brass screws. Only one of the two coaxial loops has been utilized, consisting of a single square turn of copper wire having the side a of about 1 m, according to the IEEE Std 1308-1994 recommended practice [9]. A photograph of the structure with the magnetic sensor placed at the square center is shown in Fig. 3.

The relationship between supply current i_s and flux density B_{ext} at the square center is [9]

$$\frac{B_{\text{ext}}}{i_{\text{s}}} = \frac{0.8\sqrt{2}}{a} \cong 1.14\ \mu\text{T/A}. \tag{20}$$

The working zone is limited to the volume close to the square-loop center, due to the nonuniform field distribution. In particular, inside a 10-cm cube placed in the square-loop center, the field deviation is lower than 1%. It has been analytically verified that the errors in the geometric dimensions affect the field accuracy less than 1%. Then, measuring the instantaneous value of the supply current, it is possible to calculate the corresponding flux density by (20), with a good approximation [10].

The power supply is an HP 6834B Power Source/Analyzer able to generate voltage waveform up to 5 kHz. All the supply wirings are twisted, and the power setup is kept far from the square loop to avoid magnetic-field interferences with respect to the working zone.

Fig. 3. Photograph of the Helmholtz coil realized by a wood structure. The magnetic sensor is placed at the center of one of the two square coaxial loops.

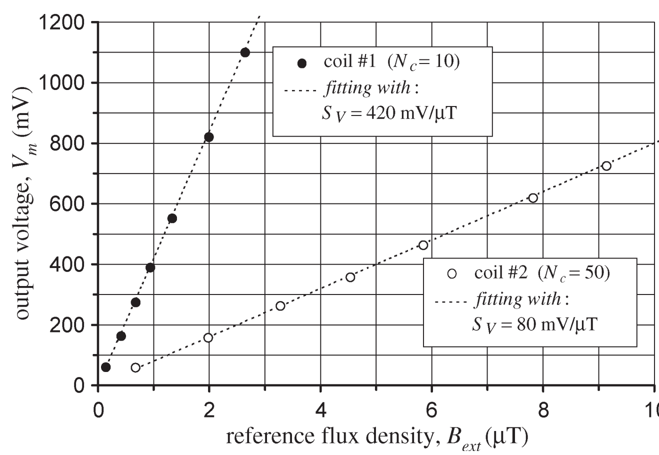

Fig. 4. Linearity test in sinusoidal steady state (50 Hz): measured data (dots) and fitting (dashed lines).

C. Experimental Tests

In order to obtain significant tests, the transducer prototype has been placed in the central working zone of the reference field-generation system, with the sensor/coil axis aligned with the square-loop axis. All the system has been horizontally oriented so that the magnetic field of the earth, i.e., about 35 μT in the Lab, resulted perpendicular to this common axis, to avoid the corresponding dc field offset. A simple high-pass filter can be also employed to cutoff the dc field components in the case of accurate ac magnetic-field measurements.

The first test consists of verifying the transducer linearity by applying a 50-Hz sinusoidal field waveform having an amplitude ranging from fractions to tens of microtesla. The results are shown in Fig. 4 for both the coils #1 and #2. The measured data are shown by dots (black and white, respectively), whereas the dashed lines represent the corresponding

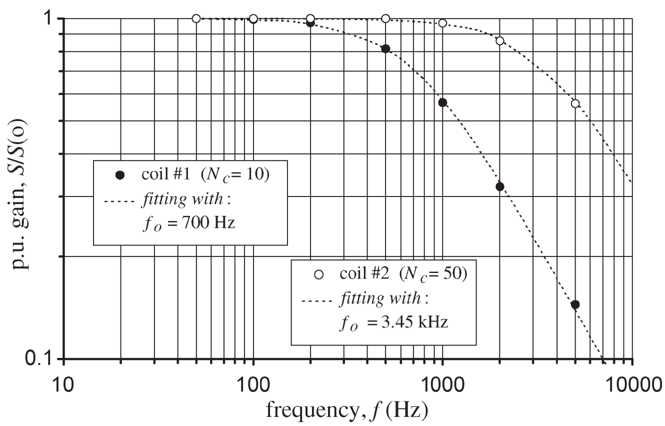

Fig. 5. Frequency response at $B_{\text{ext}} \cong 2\ \mu$T (peak): measured data (dots) and fitting (dashed lines).

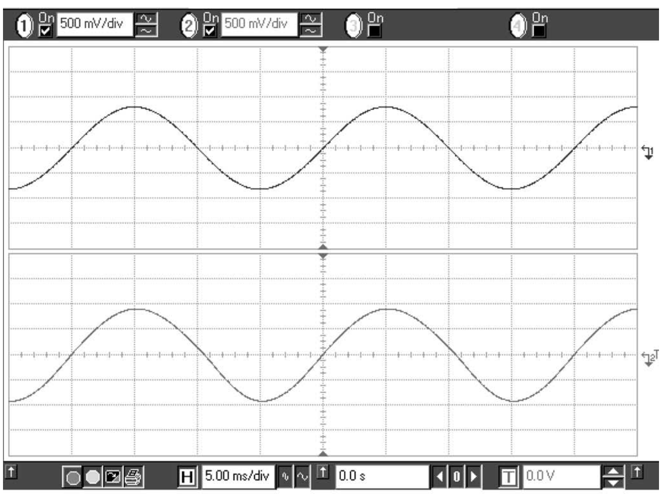

(a)

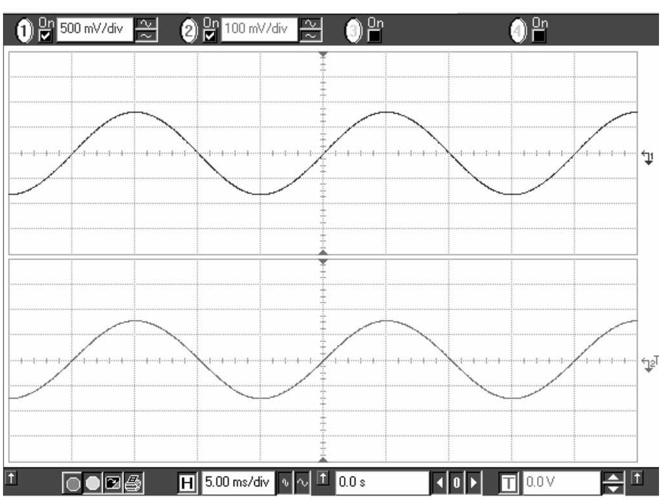

(b)

Fig. 6. Sinusoidal steady state (50 Hz). (a) Coil #1, $N_c = 10$ turns, *upper trace*: 1) reference field signal (2.43 μT/V), *lower trace*: 2) output voltage, v_m (2.38 μT/V). (b) Coil #2, $N_c = 50$ turns, *upper trace*: 1) reference field signal (2.43 μT/V), *lower trace*: 2) output voltage, v_m (12.5 μT/V).

linear fitting. The voltage sensitivities S_{V} resulting from Fig. 4 (millivolt per microtesla) confirm the calculated ones shown in Table II.

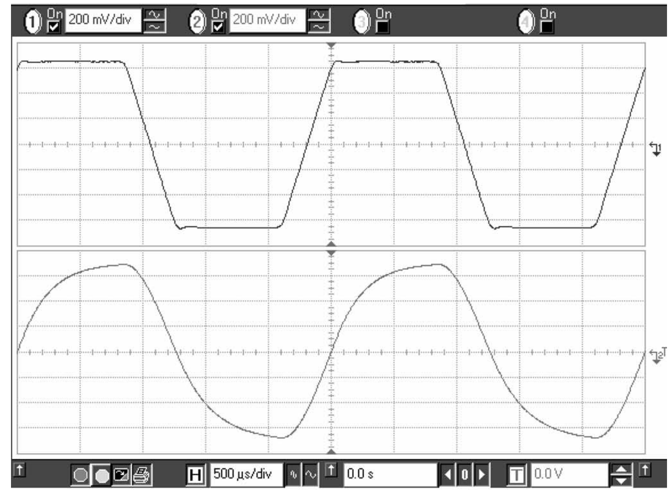

(a)

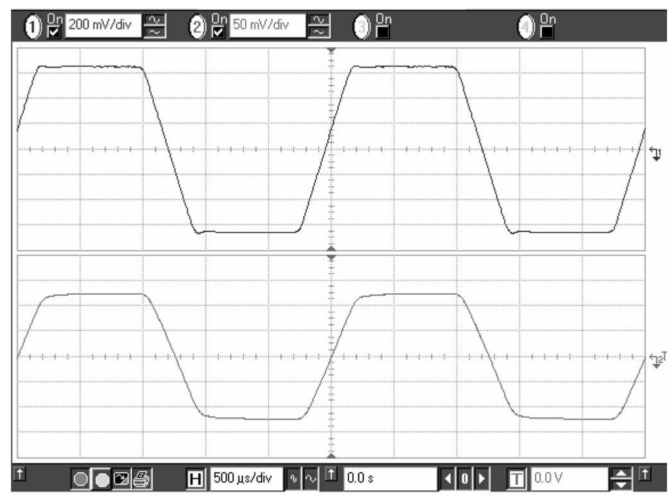

(b)

Fig. 7. Trapezoidal field waveform (400 Hz). (a) Coil #1, $N_c = 10$ turns, *upper trace*: 1) reference field signal (2.43 μT/V), *lower trace*: 2) output voltage, v_m (2.38 μT/V). (b) Coil #2, $N_c = 50$ turns, *upper trace*: 1) reference field signal (2.43 μT/V), *lower trace*: 2) output voltage, v_m (12.5 μT/V).

In Fig. 5, the frequency response of the magnetic-field transducer is shown in per unit with reference to both coils #1 and #2. Also in this case, the measured data are shown by dots (black and white), whereas the dashed lines represent the fitting on the basis of a transfer function of the first order. The resulting cutoff frequencies f_o, representing the transducer bandwidth related to the two different coils, are 700 Hz and 3.45 kHz, respectively, well inside the calculated ranges shown in Table II.

The prototype behavior considering different flux-density waveforms is shown in Figs. 6–8, for both coil #1 and coil #2.

The waveforms of the magnetic flux density are represented by the voltage drop across a 0.47-Ω resistor connected in series with the current supplying the reference-field-generation system. On the basis of (20), the resulting scaling factor is: $1.14\ (\mu\text{T/A})/0.47\ (\Omega) \cong 2.43\ (\mu\text{T/V})$.

Fig. 6 shows the sinusoidal steady-state behavior at low frequency (50 Hz), with field amplitude of about 2 μT. Figs. 7 and 8 show the prototype behavior in response to trapezoidal and rectangular field waveforms, respectively (400 Hz,

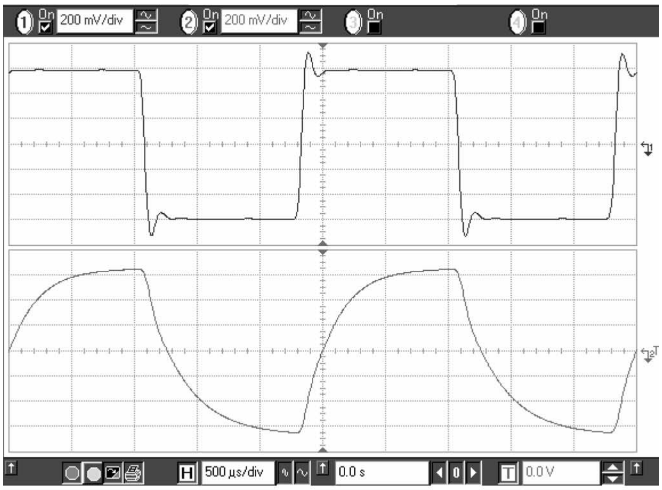

(a)

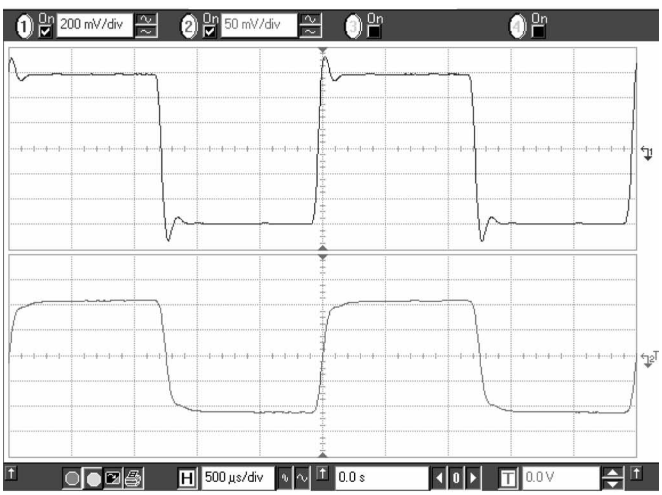

(b)

Fig. 8. Rectangular field waveform (400 Hz). (a) Coil #1, $N_c = 10$ turns, *upper trace*: 1) reference field signal (2.43 μT/V), *lower trace*: 2) output voltage, v_m (2.38 μT/V). (b) Coil #2, $N_c = 50$ turns, *upper trace*: 1) reference field signal (2.43 μT/V), *lower trace*: 2) output voltage, v_m (12.5 μT/V).

1.5 μT peak). The resulting performances emphasize the different dynamic characteristics related to coil #1 and coil #2.

In general, all the experimental tests show a satisfactory performance for the closed-loop transducer, in good agreement with the theoretical predictions.

VI. Conclusion

A magnetic-field transducer able to sense magnetic fields from dc up to tens of kilohertz has been analyzed in this paper. The closed-loop operation allows to overcome the known problems of magnetic sensors in terms of nonlinearity and thermal drift, avoiding the need for additional hardware and software compensating blocks to be included in the measuring system.

The sensitivity and the bandwidth of the transducer have been analyzed by a transfer-function approach, and a GBP has been introduced. The main advantages and disadvantages with respect to other magnetic transducers have been discussed.

A hardware prototype was realized, and the analytical developments have been verified by means of a reference magnetic-field-generation system. The resulting transducer sensitivity is very good, and flux densities in the order or fractions of microtesla can be usefully sensed in a frequency range up to tens of kilohertz. On the basis of an rms to dc converter and a millivoltmeter, a one-axis gauss meter can be readily obtained.

Useful guidelines for the transducer design are given in terms of output current and voltage sensitivity, cutoff frequency, and coil parameters.

References

[1] *IEEE Guide for the Measurement of Quasi-Static Magnetic and Electric Fields*, IEEE Std 1460-1996.

[2] J. E. Lenz, "A review of magnetic sensors," *Proc. IEEE*, vol. 78, no. 6, pp. 973–989, Jun. 1990.

[3] G. Bartington, "Sensors for low level low frequency magnetic fields," in *Proc. IEE Colloq. Low Level Low Freq. Magn. Fields*, 1994, pp. 2/1–2/9.

[4] F. Primdahl, "The fluxgate magnetometer," *J. Phys. E, Sci. Instrum.*, vol. 12, no. 4, pp. 241–253, Apr. 1979.

[5] R. J. Parker and J. C. Nowlan, "Effective magnetic measurements," in *Proc. Electr. Electron. Insul. Conf. Electr. Manuf. Coil Wind. Conf.*, Chicago, IL, 1993, pp. 215–219.

[6] G. Caruntu and O. Dragomirescu, "The nonlinearity of magnetic sensors," in *Proc. CAS*, 2001, vol. 2, pp. 375–378.

[7] J. Sedgwick, W. R. Michalson, and R. Ludwig, "Design of a digital gauss meter for precision magnetic field measurements," *IEEE Trans. Instrum. Meas.*, vol. 47, no. 4, pp. 972–977, Aug. 1998.

[8] J. M. Dias Pereira, O. Postolache, and P. M. B. Silva Girao, "A temperature-compensated system for magnetic field measurements based on artificial neural networks," *IEEE Trans. Instrum. Meas.*, vol. 47, no. 2, pp. 494–498, Apr. 1998.

[9] *IEEE Recommended Practice for Instrumentation: Specifications for Magnetic Flux Density and Electric Field Strength Meters—10 Hz to 3 kHz*, IEEE Std 1308-1994.

[10] W. M. Frix, G. G. Karady, and B. A. Venetz, "Comparison of calibration systems for magnetic field measurement equipment," *IEEE Trans. Power Del.*, vol. 9, no. 1, pp. 100–108, Jan. 1994.

Gabriele Grandi (M'00) was born in Bologna, Italy, in 1965. He received the M.Sc. (*cum laude*) and Ph.D. degrees in electrical engineering from the Faculty of Engineering, University of Bologna, Bologna, Italy, in 1990 and 1994, respectively.

In 1995, he joined the Department of Electrical Engineering, University of Bologna, as a Research Associate. Since 2005, he has been an Associate Professor. His research interests include modeling, simulation, and design of electronic power converters, with particular reference to power conditioning systems for renewable energy resources. Further topics of interest concern electromagnetic-compatibility (EMC) problems related to switching converters and circuit models of HF components. He has authored or coauthored about 60 papers published in technical journals and conference proceedings.

Marco Landini was born in Imola, Italy, in 1969. He received the M.Sc. degree (*cum laude*) in electrical engineering from the Faculty of Engineering, University of Bologna, Bologna, Italy, in 2001.

Beginning in 1996, he was a Freelance Electrical Plant Designer and Electronics Technician. In 2001, he started his teaching activity in the field of electrotechnics. Since 2005, he has been an Engineer in the Technical Staff of the Department of Electrical Engineering, University of Bologna. His activity concerns simulation, test, and design of electronic power converters, with particular reference to power-conditioning systems for renewable energy resources. Further topics of interest are EMC problems related to power lines and electrical stations.